Supporting Information:

Specificity and Synergy at the Oil-Brine interface: New Insights from Experiments and Molecular Dynamics Simulations

Safwat Abdel-Azeim [a]*, Sivabalan Sakthivel [a], Tarek A. Kandiel [b], and Mazen Y. Kanj [a]

[a] Center for Integrative Petroleum Research (CIPR), College of Petroleum Engineering and Geosciences, King Fahd University of Petroleum and Minerals (KFUPM), Dhahran 31261, Saudi Arabia.

[b] Department of Chemistry, King Fahd University of Petroleum & Minerals (KFUPM), Dhahran 31261, Saudi Arabia

*Corresponding author: Safwat Abdel-Azeim: abdelazeim@kfupm.edu.sa

Table S1: SARA compositional analysis and TAN of the crude oil.

SARA fractional analysis (wt%)	
Saturates	32.8
Aromatics	50.0
Asphaltene	2.8
Resin	11.0
Total acid number (TAN)	
6.5 mg KOH/g oil	

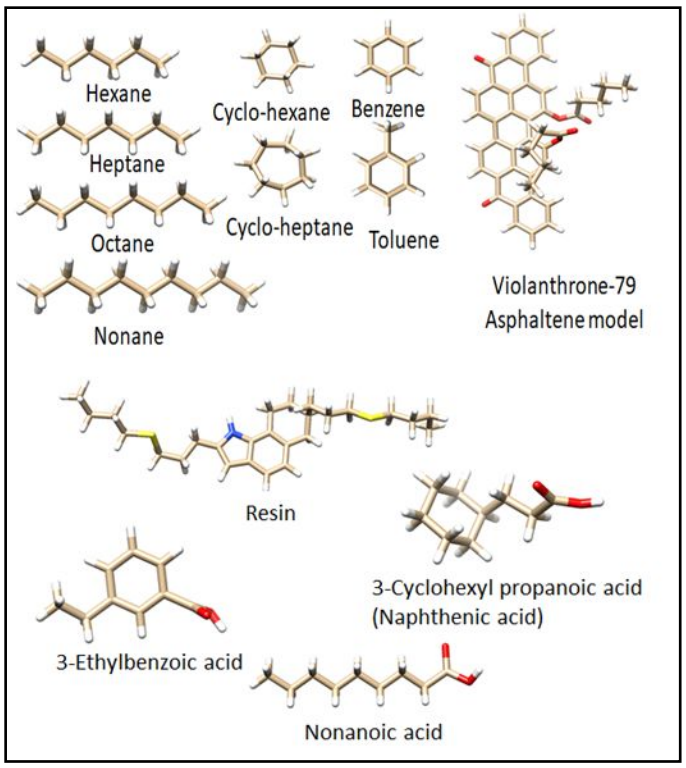

Figure S1: Molecular structures of the crude-oil components (saturates, aromatics, asphaltene, and resin) used in our MD simulations.

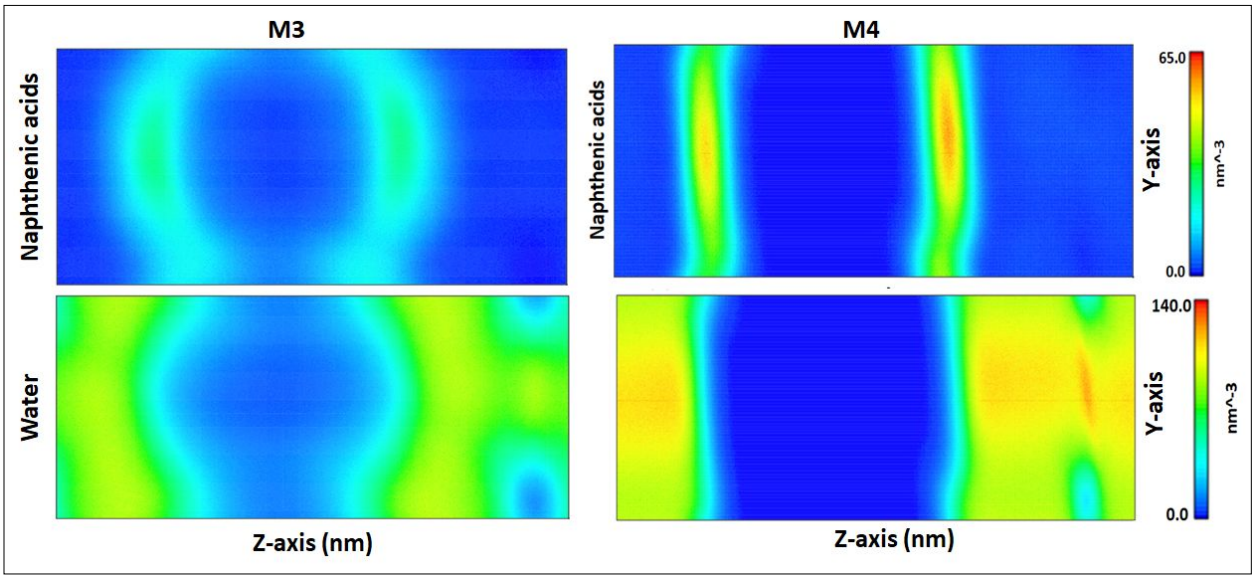

Figure S2: 2D number density map of the organic acids in xy plane and average along the z-axis.

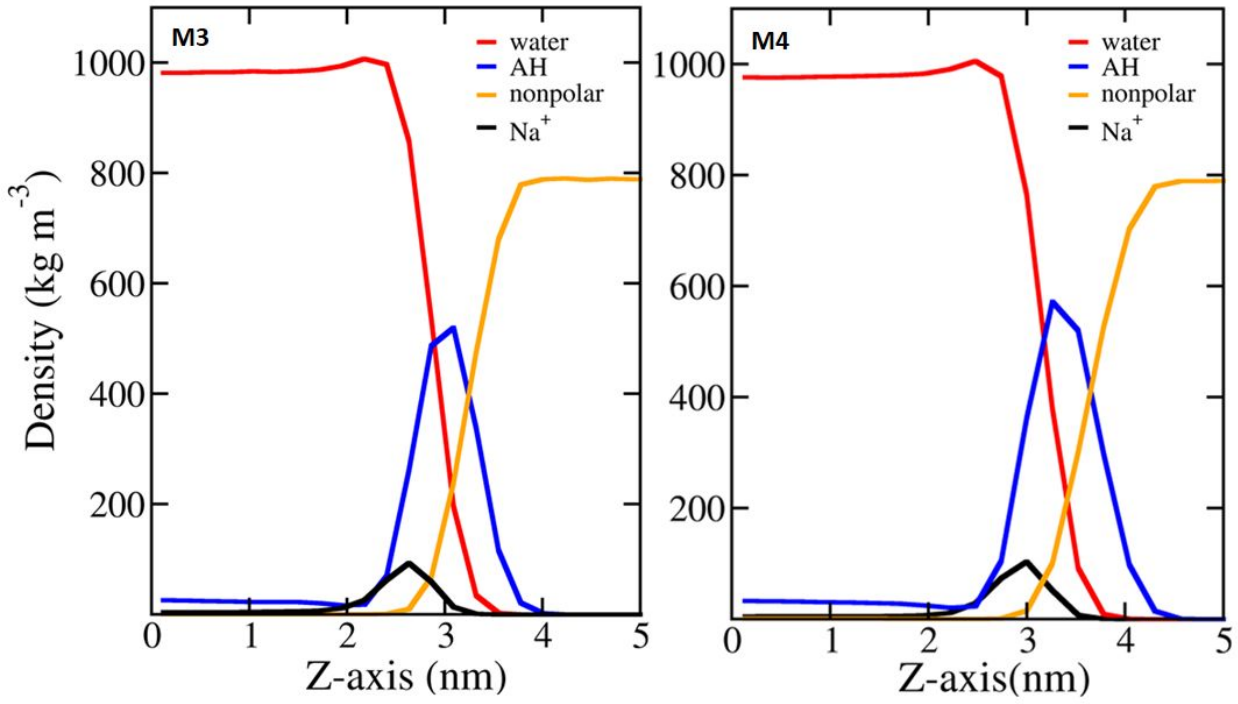

Figure S3: The partial density of the main componenents of the two phases in the xy plane and is averaged along the z-axis. Nonpolar is all the oil phase except the organic acids.

Table S2: Total IFT (mN/m) averaged over 200-500 ns period of MD simulations for oil: sea, formation and 50% diluted formation waters interfaces using M4 oil model.

	Average IFT (mN/m)		
	SW	50%FW	FW
Exp.	28.65 ±0.30	32.75±0.40	36.70±0.30
M4	26.25± 0.35	35.68 ± 0.18	39.88 ± 0.15

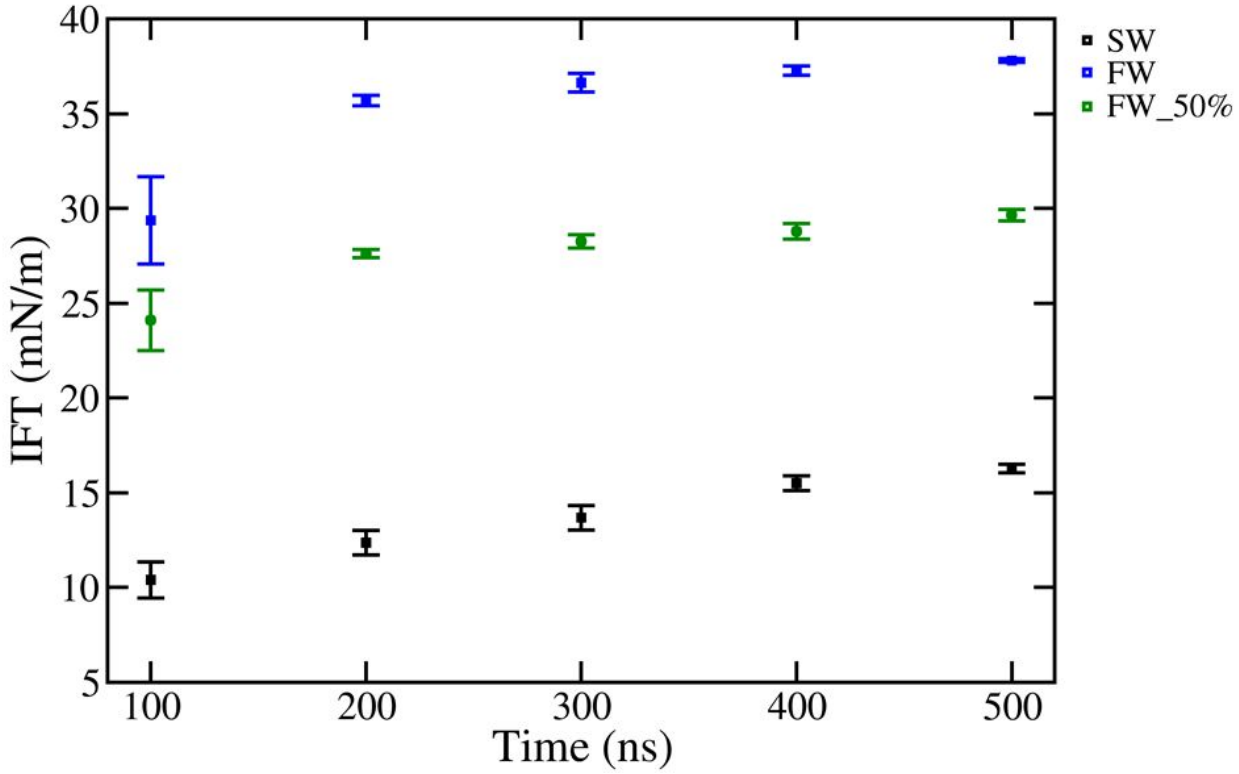

Figure S4: IFT of of sea, formation, and 50% diluted formation waters as a function of time calculated for models M5.

Table S3: Total IFT (mN/m) averaged over 200-500 ns period of MD simulations for oil: sea, formation and 50% diluted formation waters interfaces using M5 oil model.

	Average IFT (mN/m)		
	SW	FW	50% FW
M5	14.45 ± 0.48	36.86 ± 0.28	28.58 ± 0.32

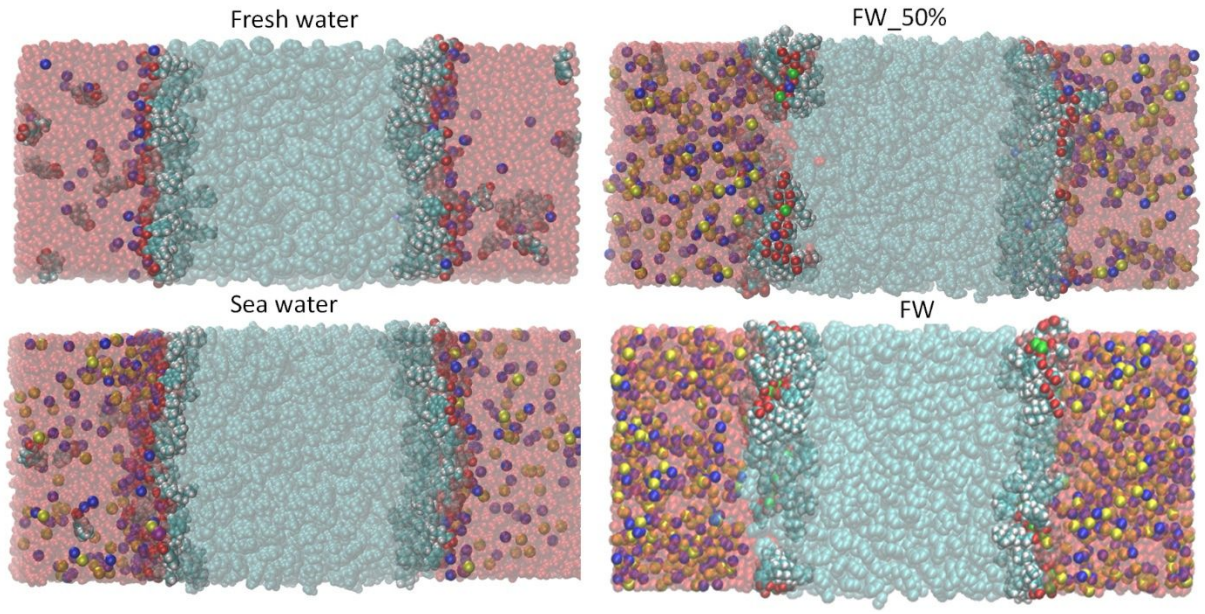

Figure S5: 500ns snapshot of oil:brine interface for freash, sea, FW_50%, and FW systems using oil model **M4**. The Organic acids, oil, ions, and water are shown in spheres. Colode code: O:red, C:cyan, H:white, Na^{+}:blue, Ca^{2+}:green, Mg^{2+}:purple, and Cl-:yellow.

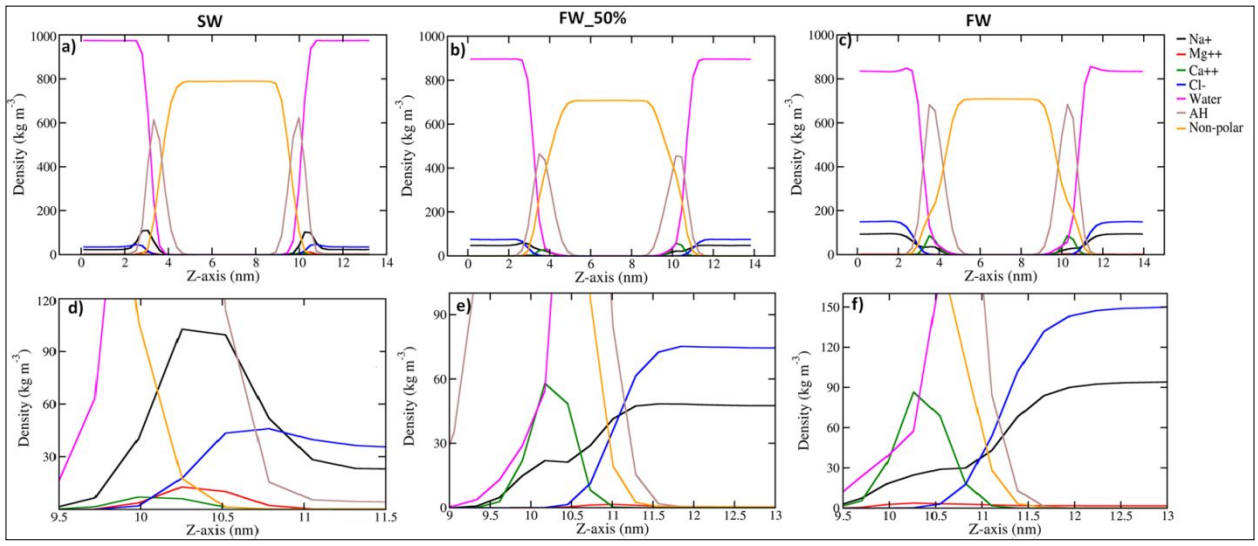

Figure S6: Partial density along Z-axis of the simulation box of oil and brine components (a, b, and c). d, e, and f are zoom in at the oil:brine interface.

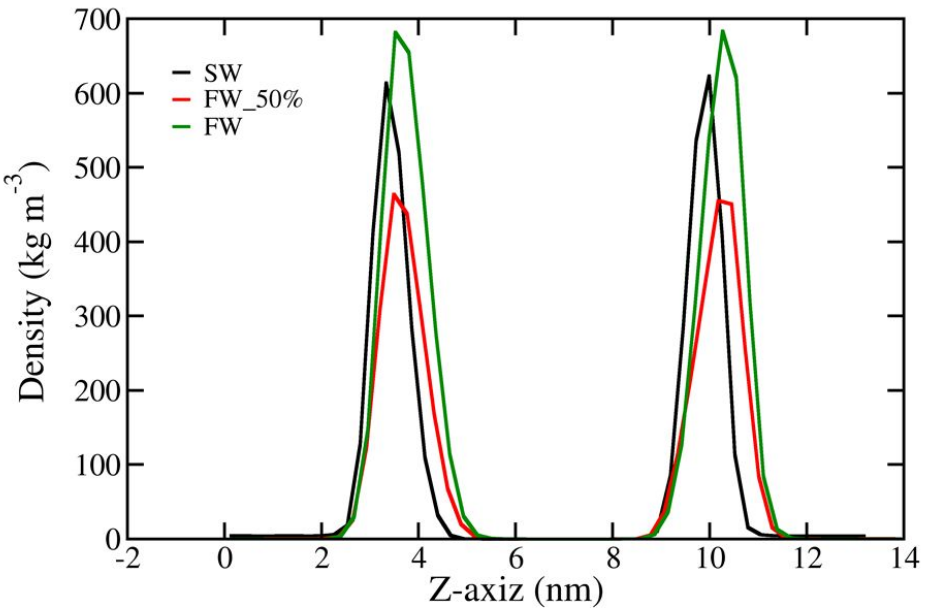

Figure S7: Partial density along Z-axis of the simulation box of the organic acids calculated for the three considerd brines.

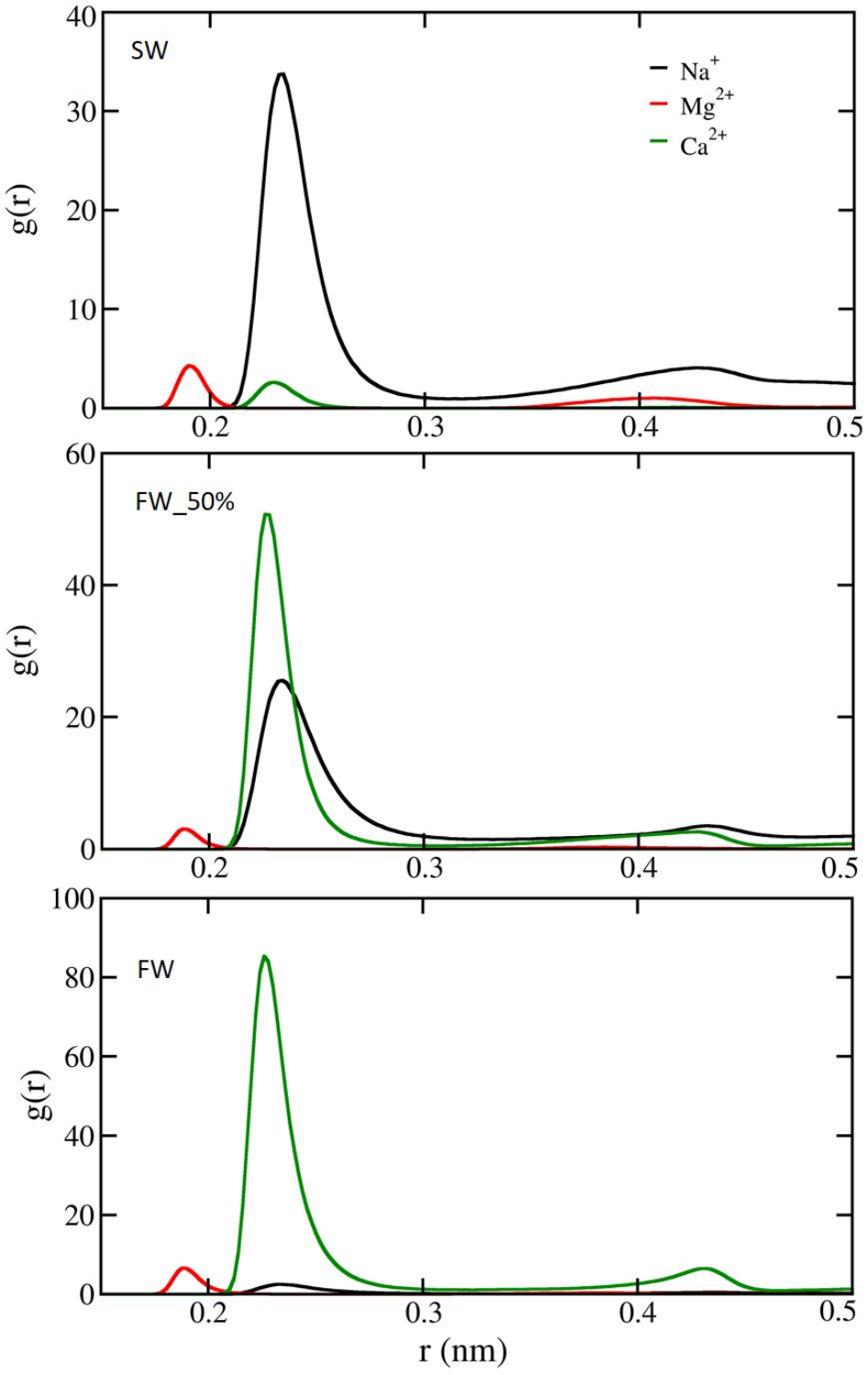

Figure S8: Radial distribution functions between the organic acids and the different ions in the brine solutions.

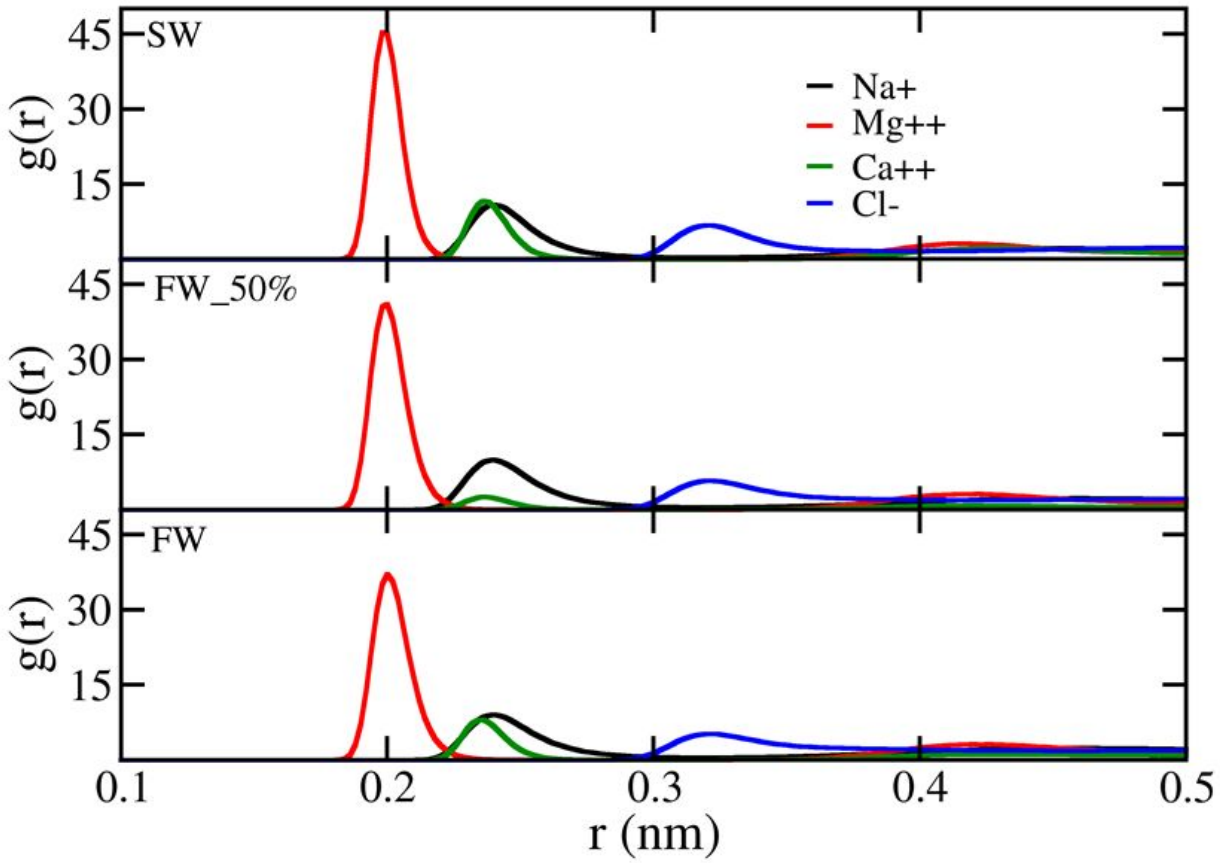

Figure S9: Radial distribution functions between water (OW) and the different ions in the brine solutions calculated for the three brine compositions considered in our stury.

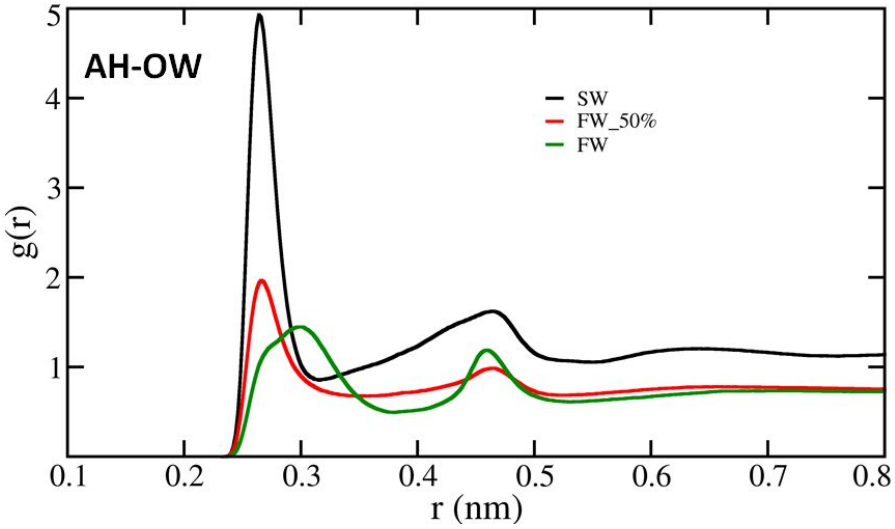

Figure S10: Radial distribution function between the organic acids head group (oxygen atoms) and water show the degree of head group hydration as a function of the salinity gradient.

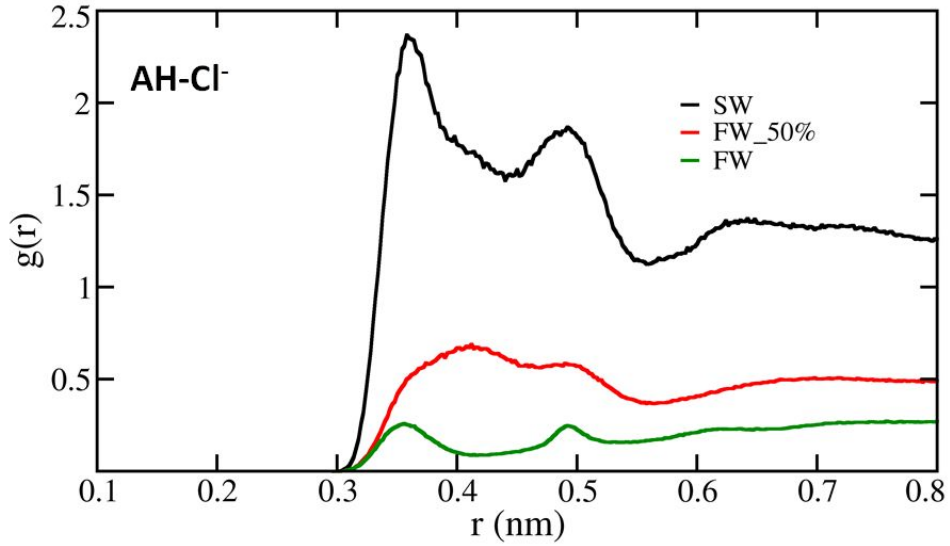

Figure S11: Radial distribution function between the organic acids head group (oxygen atoms) and chloride anions show the degree of Cl- accumulation on the surface of the organic acids.

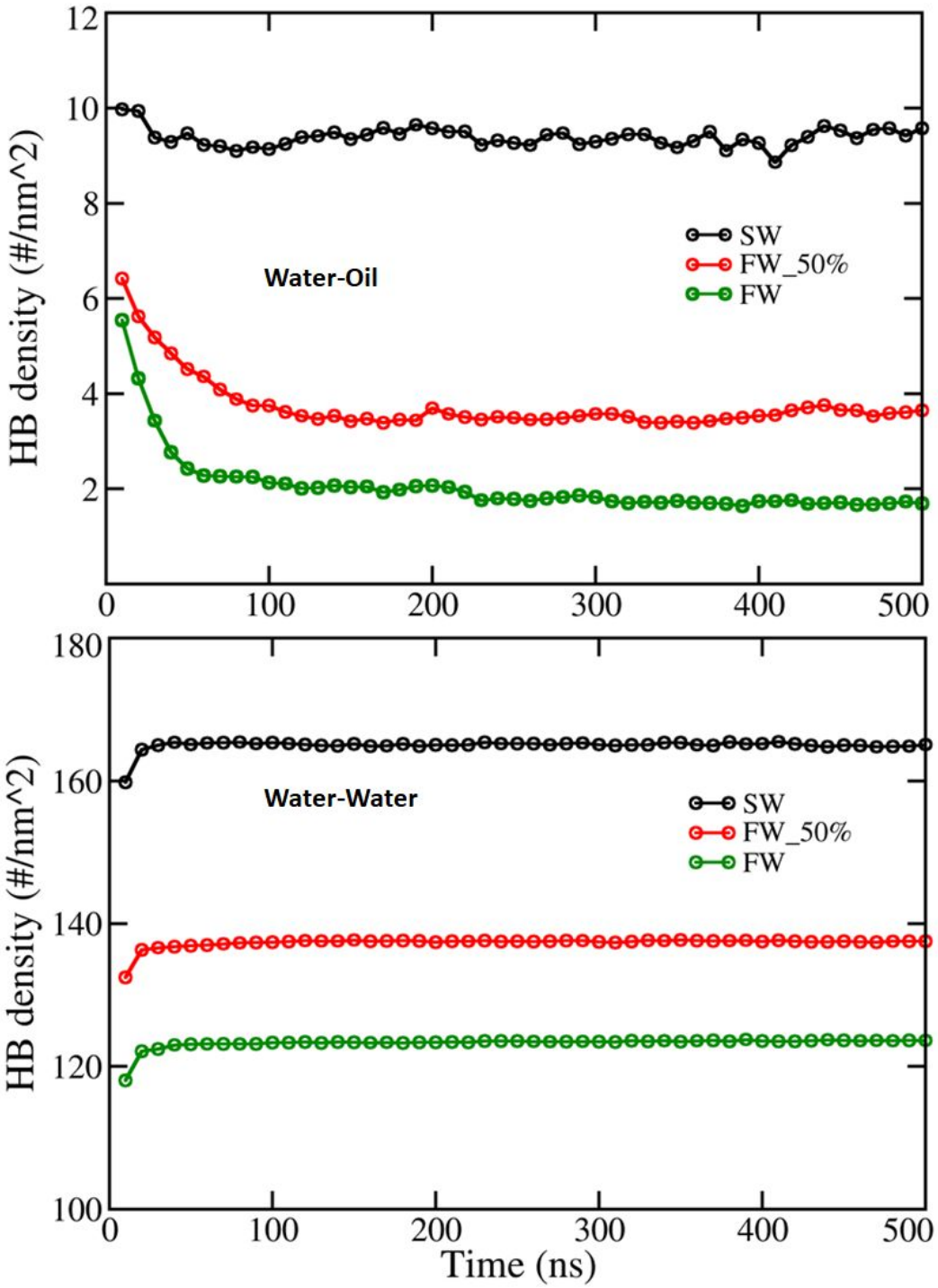

Figure S12: Hydrogen bond density (number of HB per area of interface) for oil-water and water-water interactions.

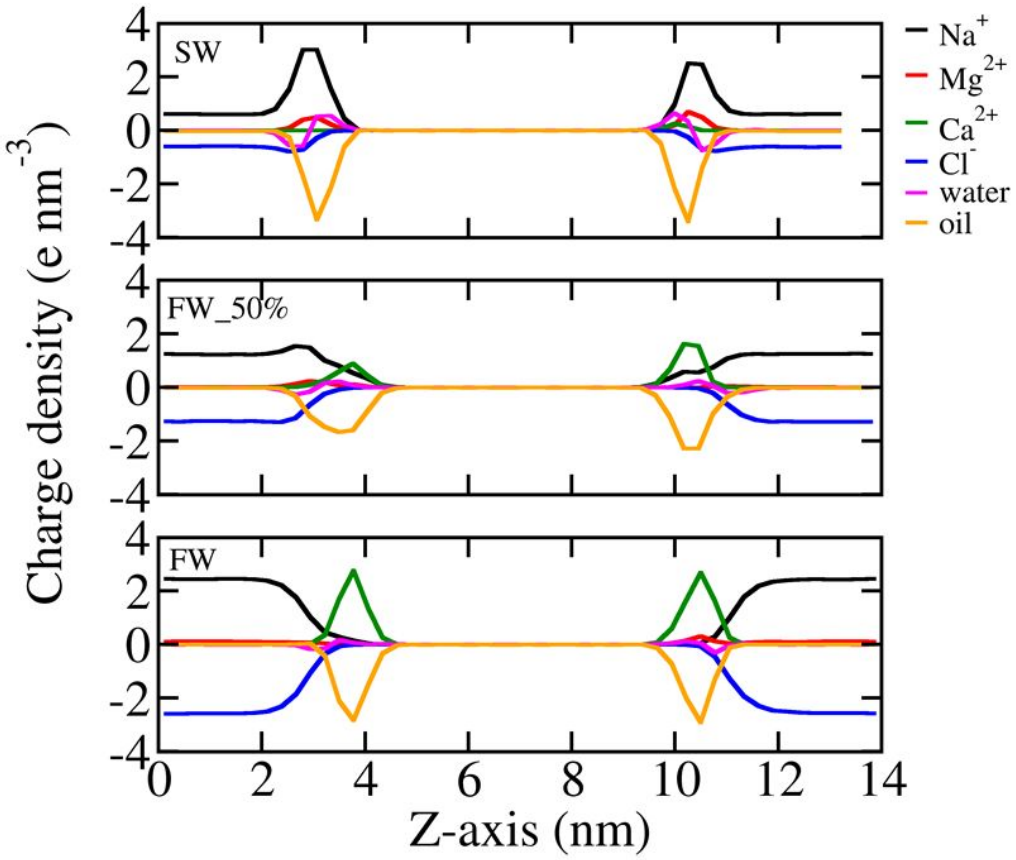

Figure 13: Charge desnity distributions for the different oil and brine components calculated for sea, formation, and 50% diluted formation waters. The charges are average over 30 slices along the Z-axis of the simulation box, which is perpendicular to the interface plane.

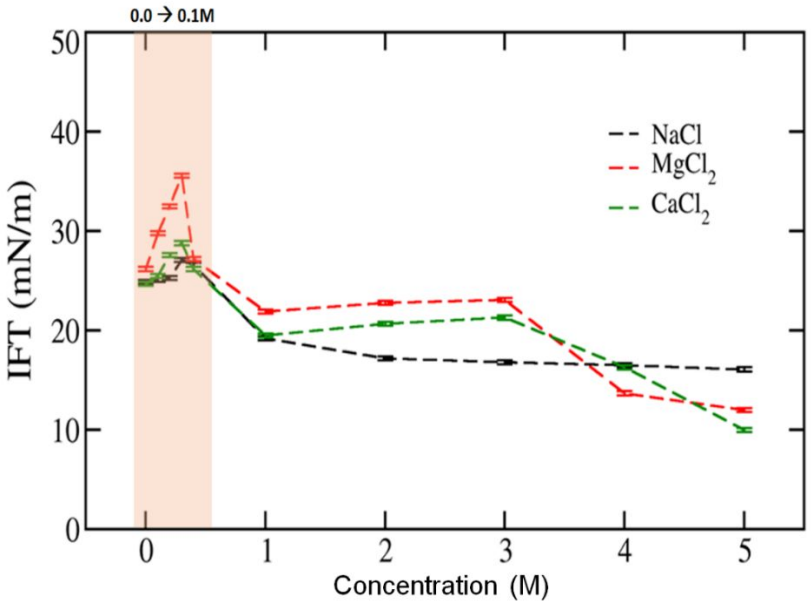

Figure S14: Interfacial tension of oil-brine solutions of the indvidual salts (NaCl, MgCl2, CaCl2) as a function of their molar concentrations. The low range concetrations are 0.0, 0.1, 1.0, and 10.0 mM.

Table S4: Experimental IFT of oil:brine systems of the different individual salts considered in our study at 10 concentration series.

Conc. (M)	0.00001	0.0001	0.001	0.01	0.1	1	2	3	4	5
NaCl	24.9	25.1	25.3	27.1	26.6	19.2	17.2	16.8	16.5	16.1
CaCl2	24.7	25.5	27.6	28.8	26.2	19.5	20.7	21.3	16.3	10
MgCl2	26.2	29.8	32.5	35.6	27.2	21.9	22.8	23.1	13.7	12

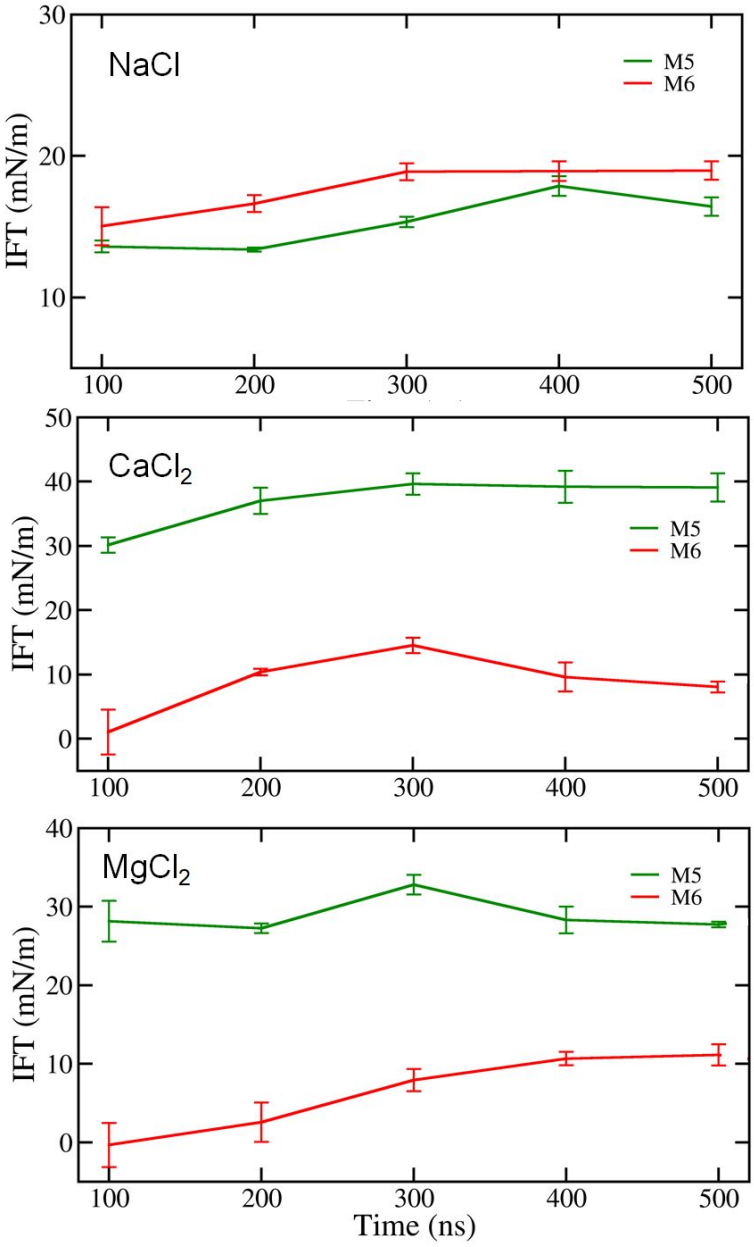

Figure S15: Interfacial tension of oil-brine solutions of the indvidual salts (NaCl, CaCl2, and MgCl2) as a function of time at 5M salt concentrations.

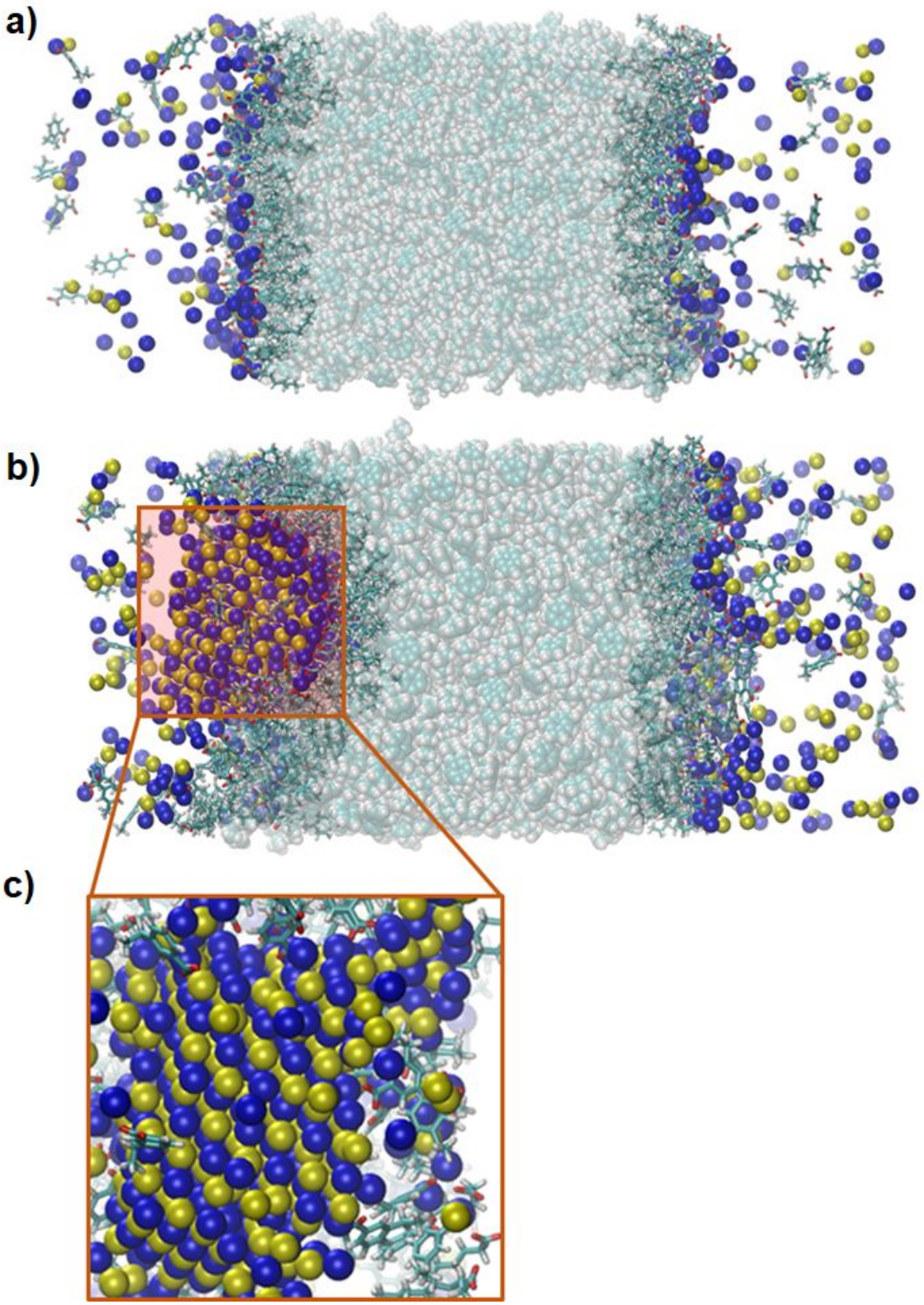

Figure S16: Oil-water interfaces for NaCl at 2M concentration (a) and at 5M concentration (b,c). Ions are represented by spheres. Organic acids are shown in sticks. we removed water for the sake

of clarity. Crude oil is represented by Vand der waals spheres. Color code; H:white, O:red, C:cyan, Na_+:blue, Cl-:yellow, Ca^{2+}:green, Mg^{2+}:purple. Crude oil simulated using M6.

S17: Further analysis of the individual oil-brine interfaces.

NaCl-brine interface:

The partial mass and charge densities are shown in Figures S18, S19 demonstrate the growth of NaCl crystal at the interface. Also, the radial distribution function g(r) between Na^+ and Cl^- clearly shows the short and long-rang ordering of NaCl crystallites (Figure S20). Further, at 5M of NaCl, the hydrogen bonds between the oil-water and the water-water are increasing, which is a sign of NaCl crystal formation (Figure S18). In addition, a lamellar structure is formed at 2M NaCl with the **M6** oil model. Using oil model **M5** at the same salt concentration, IFT decreases, and diverges from the experimental value. The difference between **M5** and **M6** oil models is the addition of the chloride ions in **M6**. The amount of Na^+ required to neutralize the deprotonated organic acids is already at 2M concentration in **M5**. At this low concentration, we observed a clear salting-in effect by the dissolution of the organic acids into the aqueous phase.

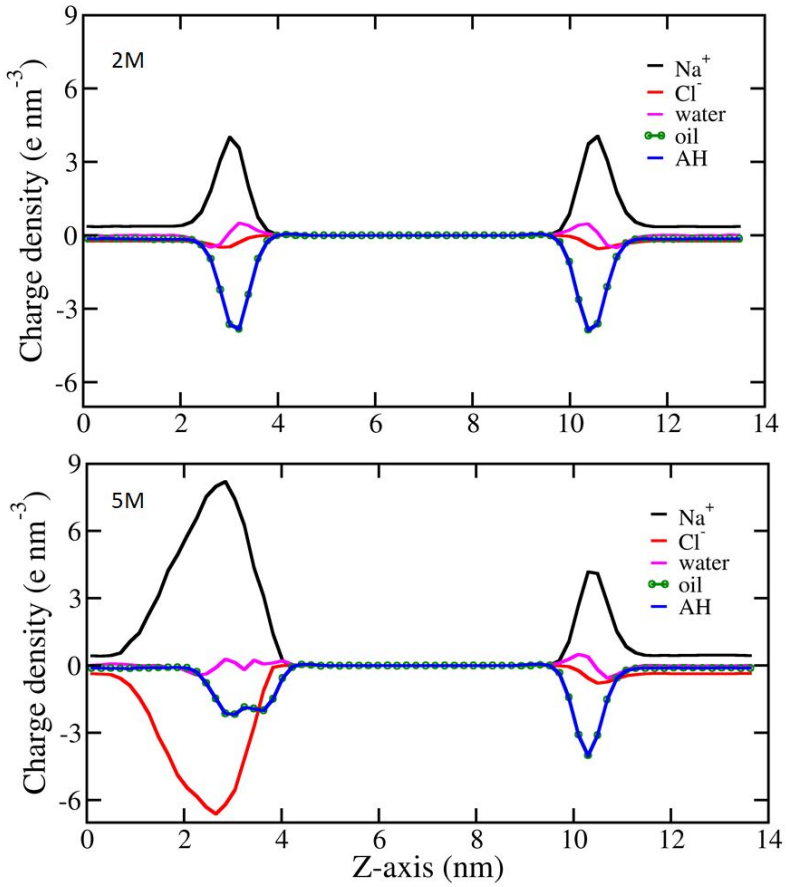

Figure S18: Charge density along Z-axis (normal to the interface) for the brine ions (Na+, and Cl-), water, oil, and organic acids for 2- and 5M concentrations of NaCl.

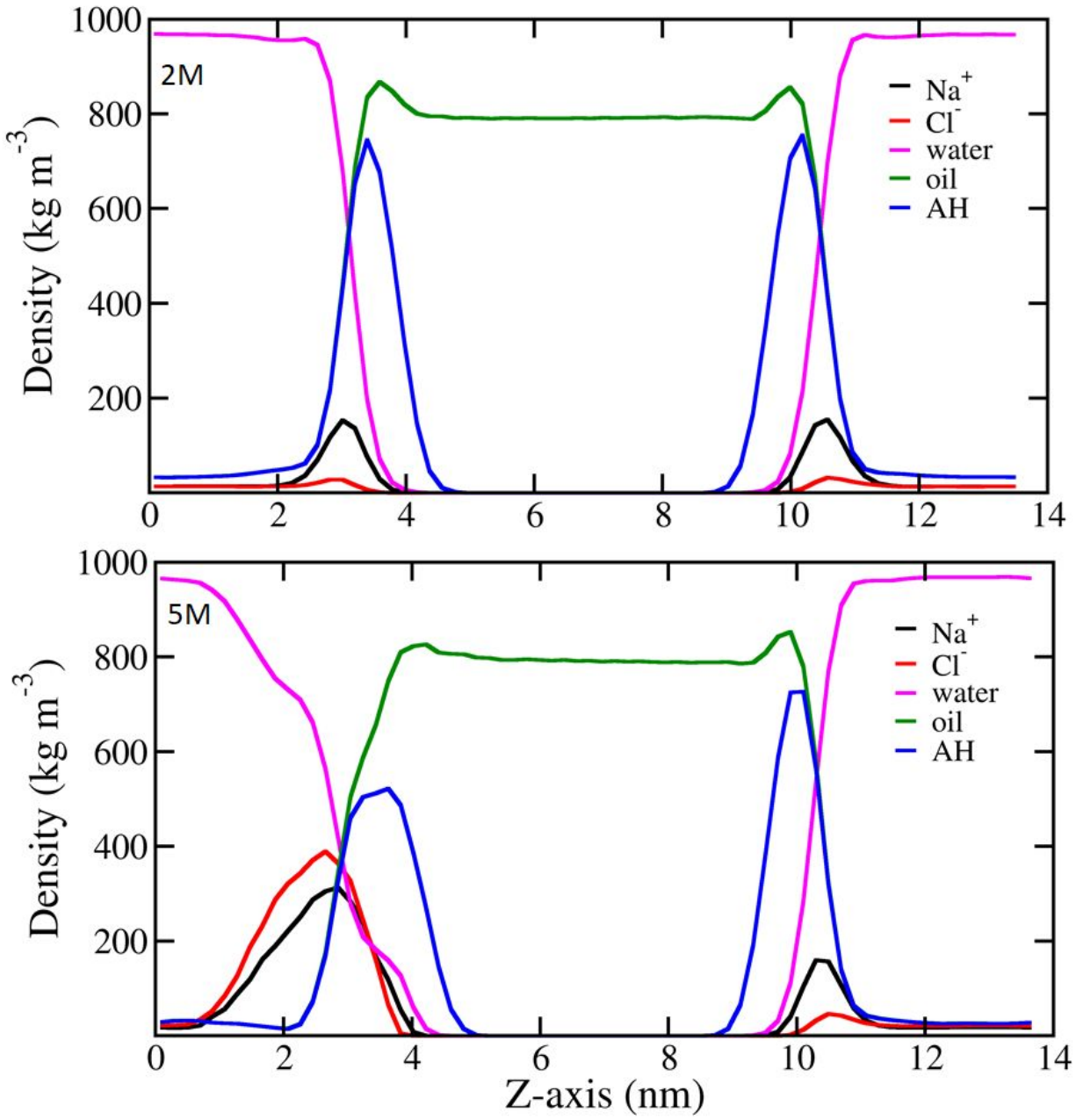

Figure S19: partial mass density along Z-axis (normal to the interface) for the brine ions (Na+, and Cl-), water, oil, and organic acids for 2- and 5M concentrations of NaCl.

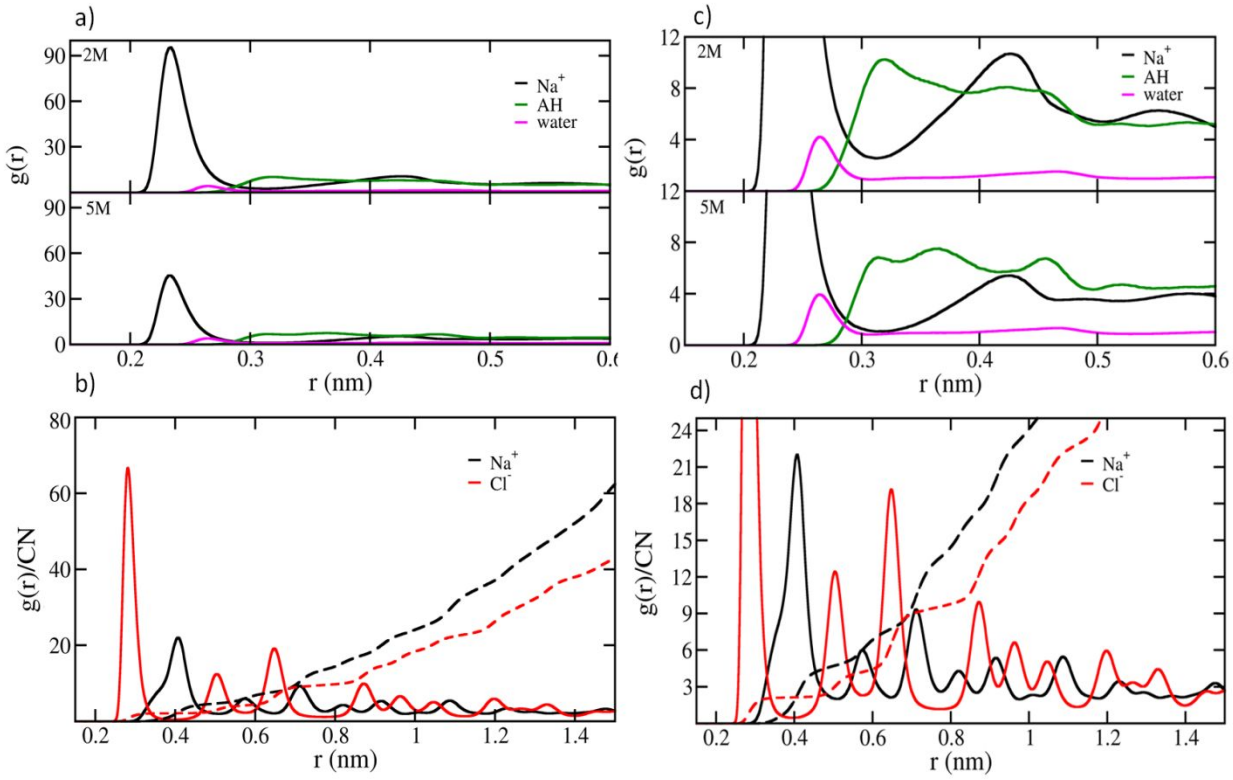

Figure S20: Radial distribution functions g(r) calculated between the oxygen of the organic acids with Na+, water, and themselves (a, c). g(r) between Na+ with Na+, and Cl- for 5M brine solution. c & d are zoom in of g (r) ploted in a & b.

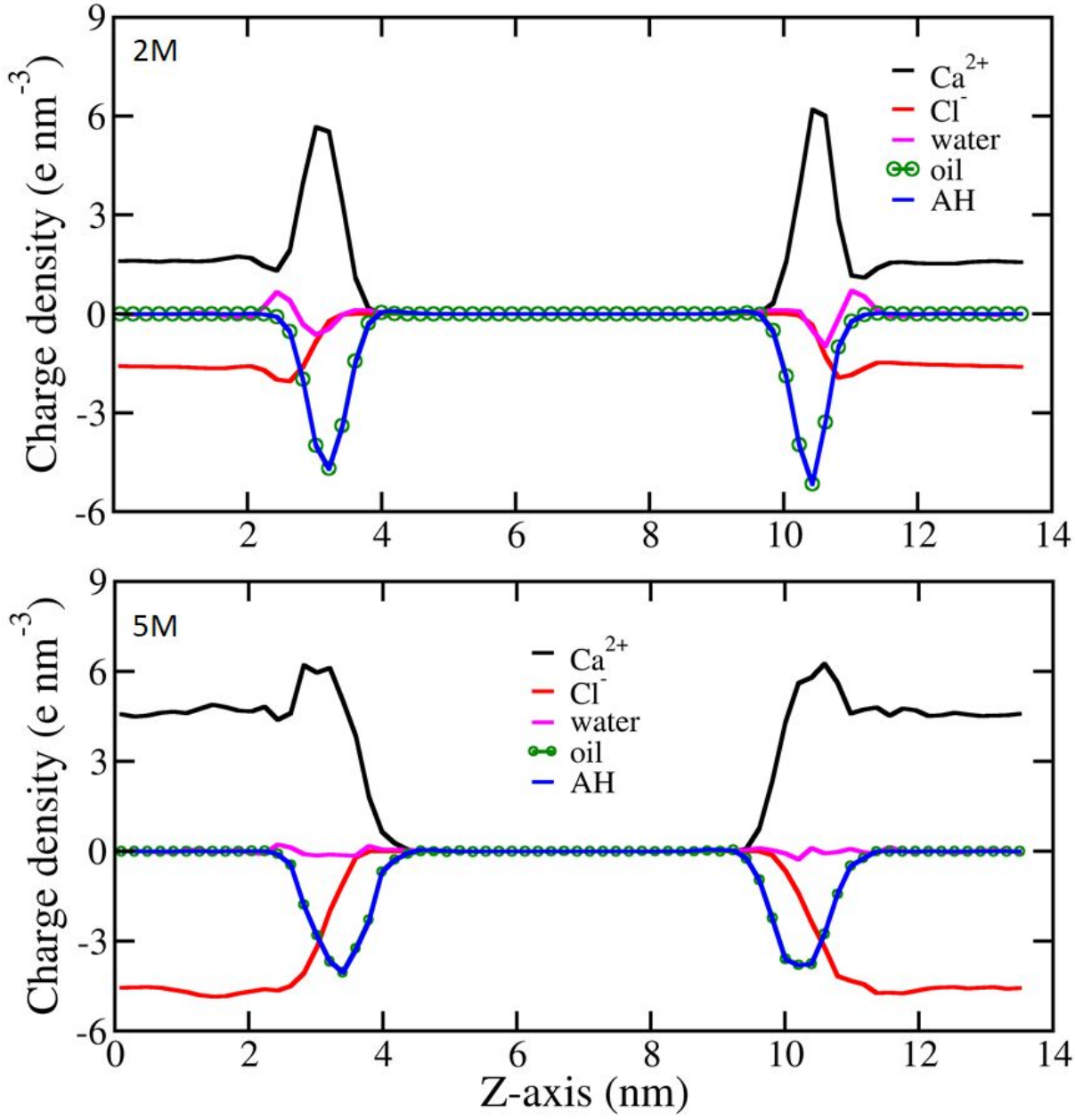

Figure S21: Charge density along Z-axis (normal to the interface) for the brine ions (Ca2+, and Cl-), water, oil, and organic acids for 2- and 5M concentrations of CaCl2.

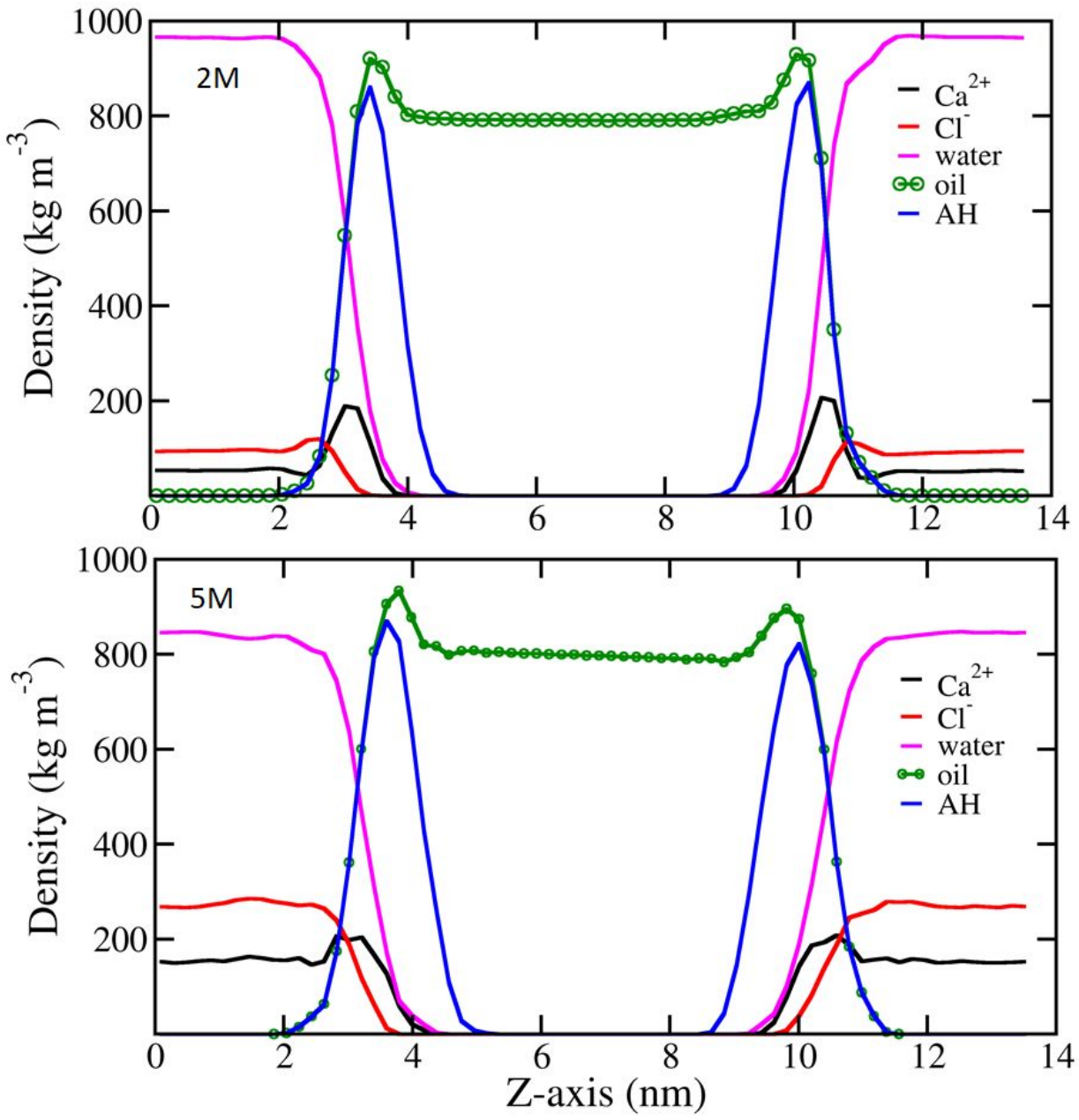

Figure S22: partial mass density along Z-axis (normal to the interface) for the brine ions (Ca^{2+}, and Cl^-), water, oil, and organic acids for 2 and 5M concentrations of $CaCl_2$.

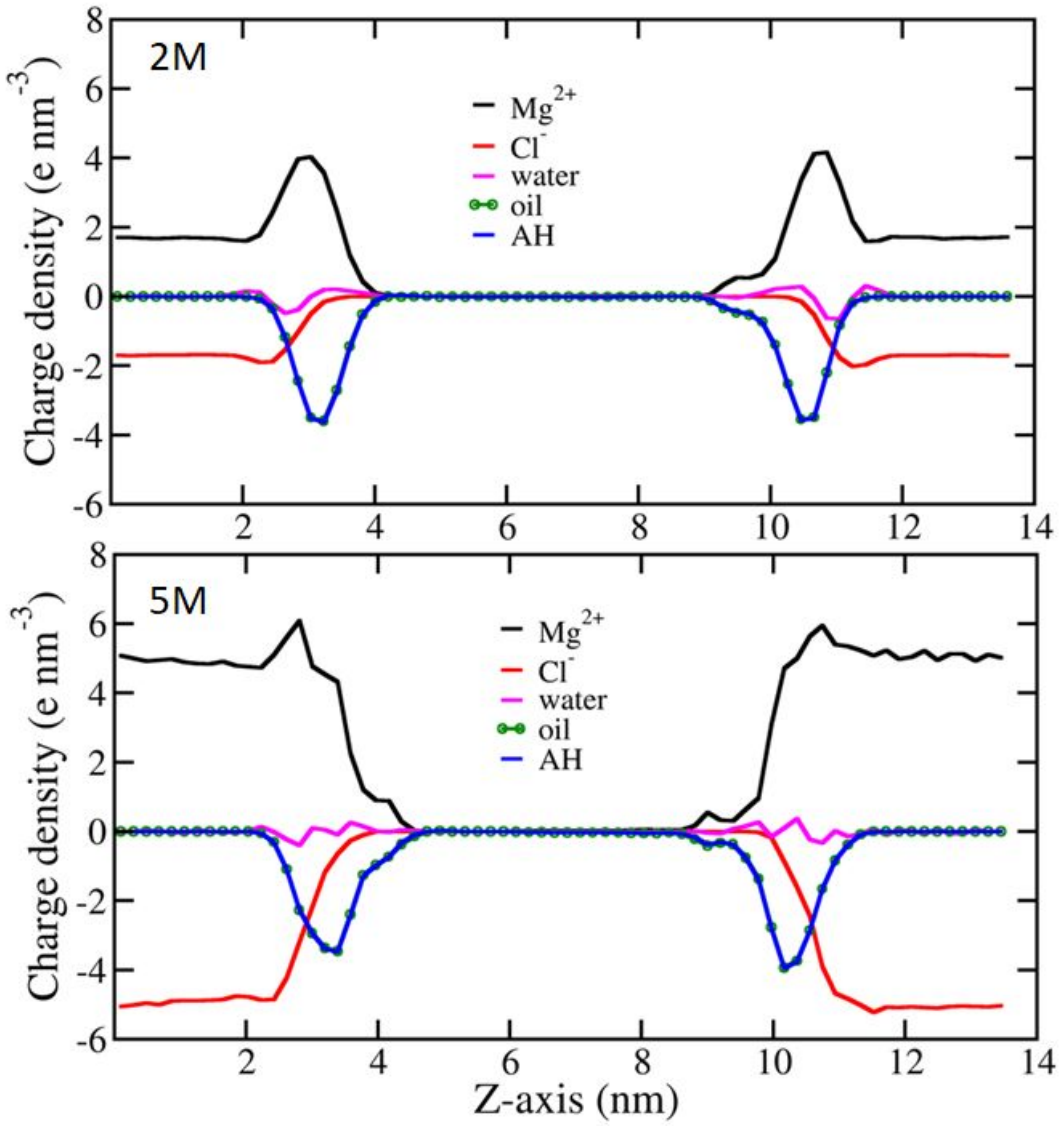

Figure S23: Charge density along Z-axis (normal to the interface) for the brine ions (Mg^{2+}, and Cl^{-}), water, oil, and organic acids for 2- and 5M concentrations of $MgCl_2$.

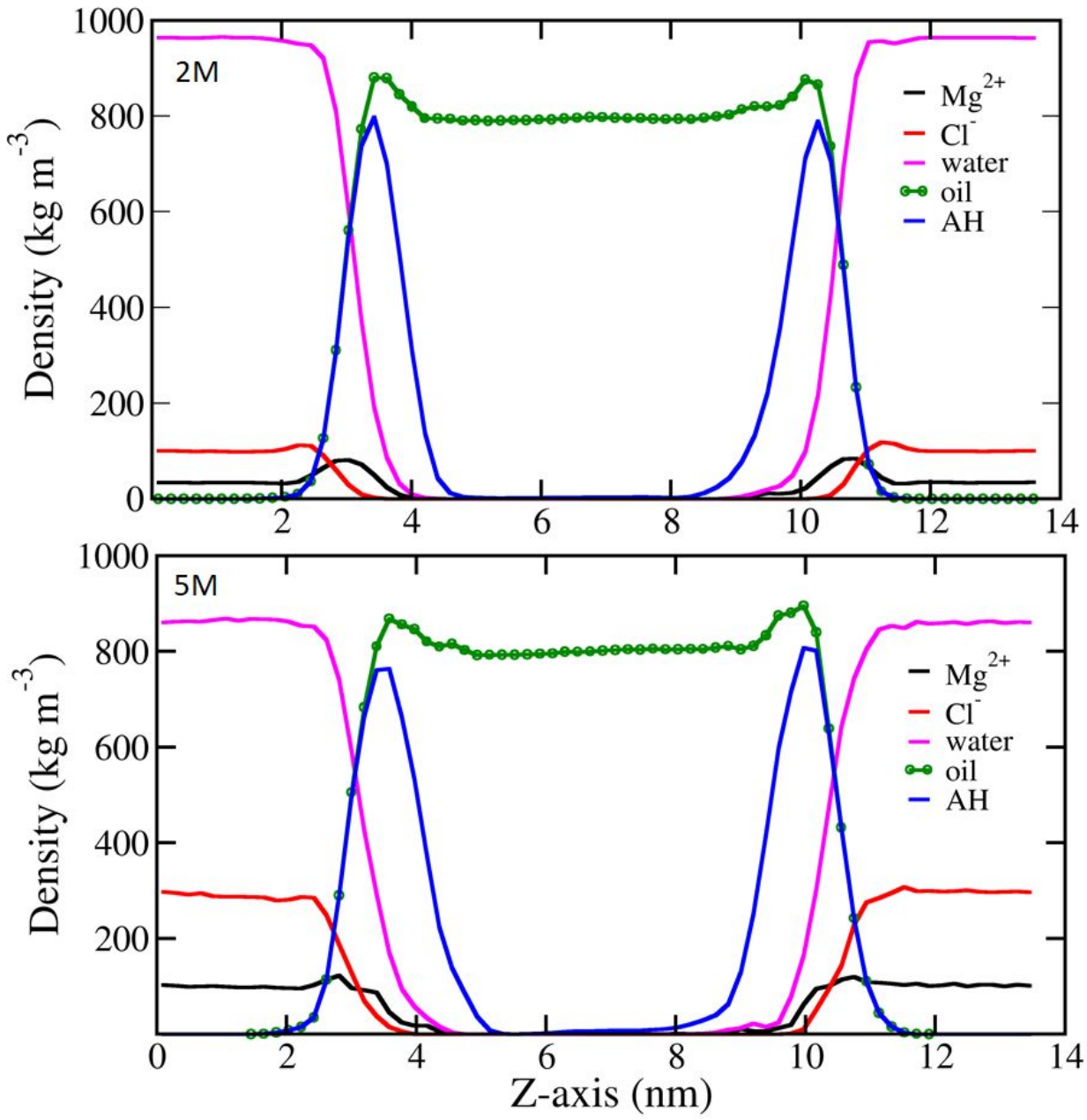

Figure S25: Partial mass density along Z-axis (normal to the interface) for the brine ions (Mg^{2+}, and Cl^-), water, oil, and organic acids for 2 and 5M concentrations of $MgCl_2$.

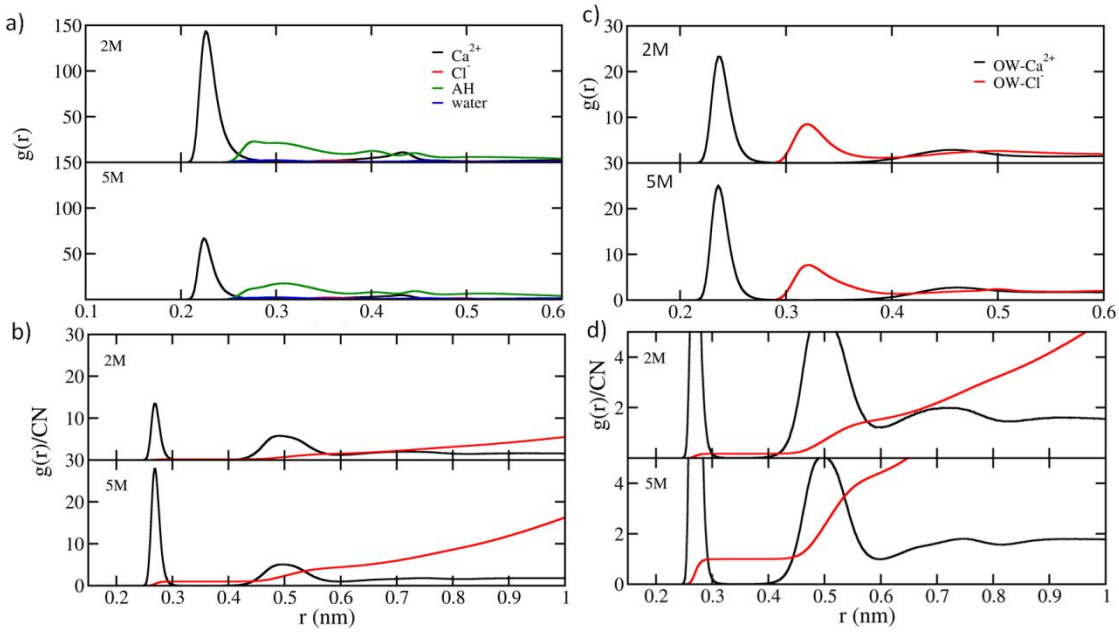

Figure S26: Radial distribution functions g(r) calculated between the oxygen of the organic acids with Ca^{2+}, water, and themselves (a). b) g(r) and coordination number between Ca^{2+}, and Cl^- (d) is a zoom in of b). c) is g(r) between water and Ca^{2+}, and Cl^- ions.

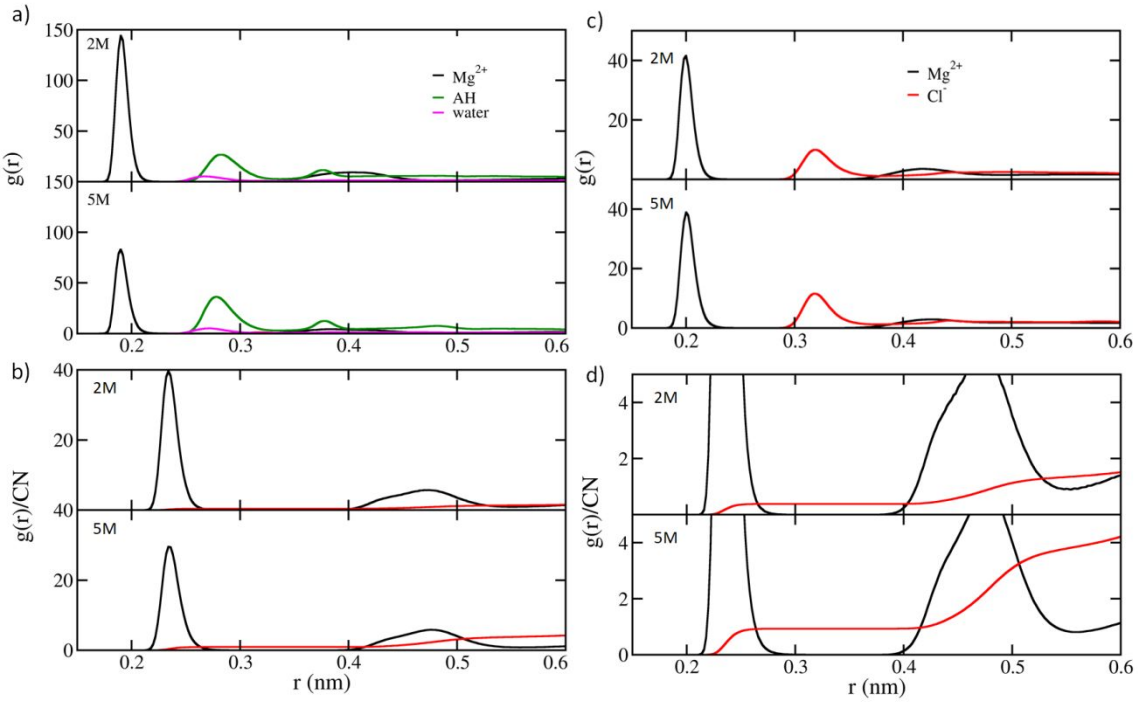

Figure S27: Radial distribution functions g(r) calculated between the oxygen of the organic acids with Mg^{2+}, water, and themselves (a). b) g(r) between Mg^{2+} and Cl^- for 2, and 5M brine solution. d) is zoom in of g (r) ploted in b. c) is the g(r) between OW of water and Mg^{2+} and Cl^- ions.

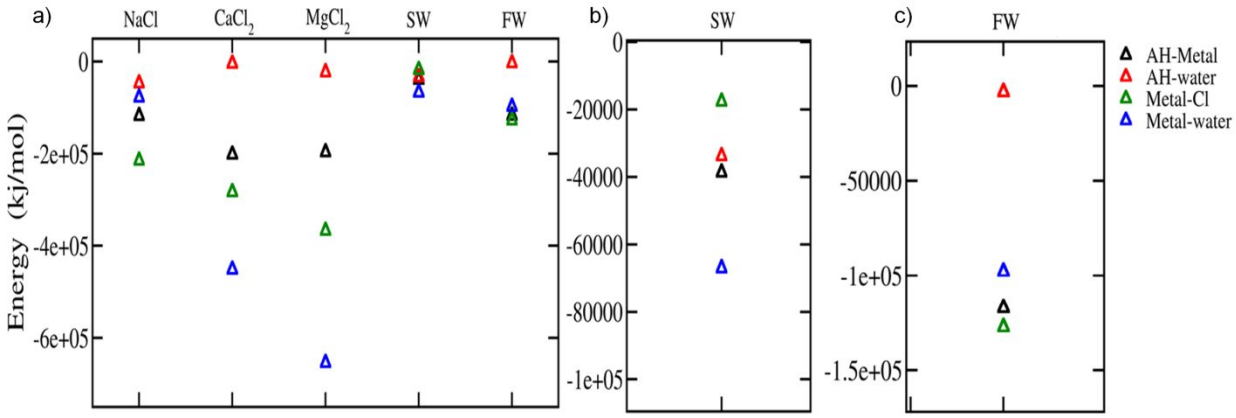

Figure S28: Molecular interaction eenrgies between the organic acids and the ionic compositions of different electrolyte solutions at 5M concentration. b) & c) are zoom in for the sea (SW), and formation (FW) waters.

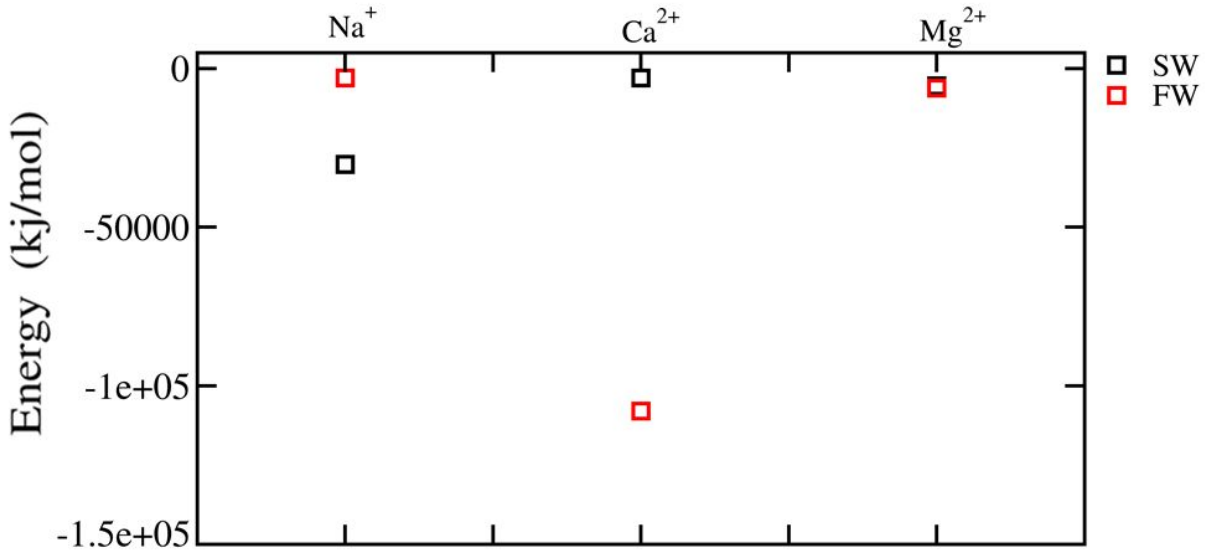

Figure S29: The individual metal ion contribution to the total metal-organic acid interaction energies in the sea and formation waters (depicted in Figure S24).

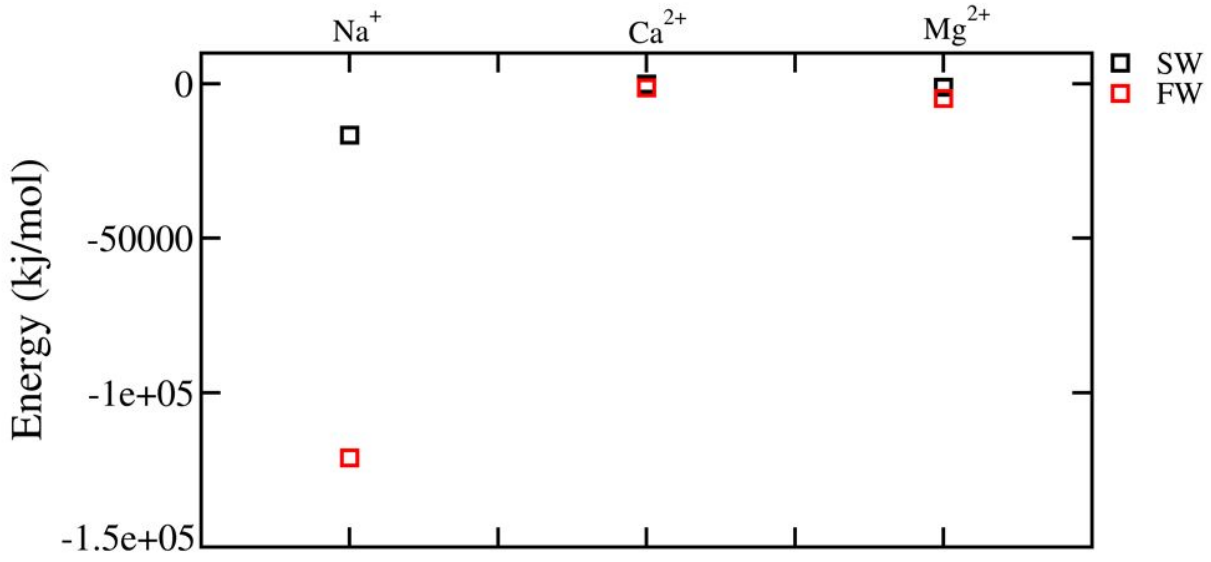

Figure S30: The individual metal ion contribution to the total metal-Cl^- interaction energies in the sea and formation waters (depicted in Figure S25).

S31: Oil-brine interface in the absence of organic acids

We further conducted MD simulations of the oil-brine interface for the mon-ovalent (Na^+) and divalent (Ca^{2+}) ions in the absence of the organic acids to examine their role on the oil-brine IFT. This organic-acids-free system is abundant in the literature. We simulated four concentrations similar to those performed in the presence of organic acids for comparison. Figure S28 presents the typical IFT trend found in the literature of oil-brine system using decane as an oil model. At low concentrations, NaCl and $CaCl_2$ behave similarly. At high concentrations, $CaCl_2$ displays a much higher effect on IFT than NaCl. In the case of NaCl, IFT fluctuates around a value of 45.0 mN/m, which is lower than the typical IFT of a fresh water-hydrocarbon system. In the case of $CaCl_2$, IFT reaches its maximum value of 61.0 mN/m at a 5M concentration. The IFT trends of both salts are well correlated to their capacity to modify the water structure at the interface due to their coordination chemistry properties as commonly observed in biochemistry.

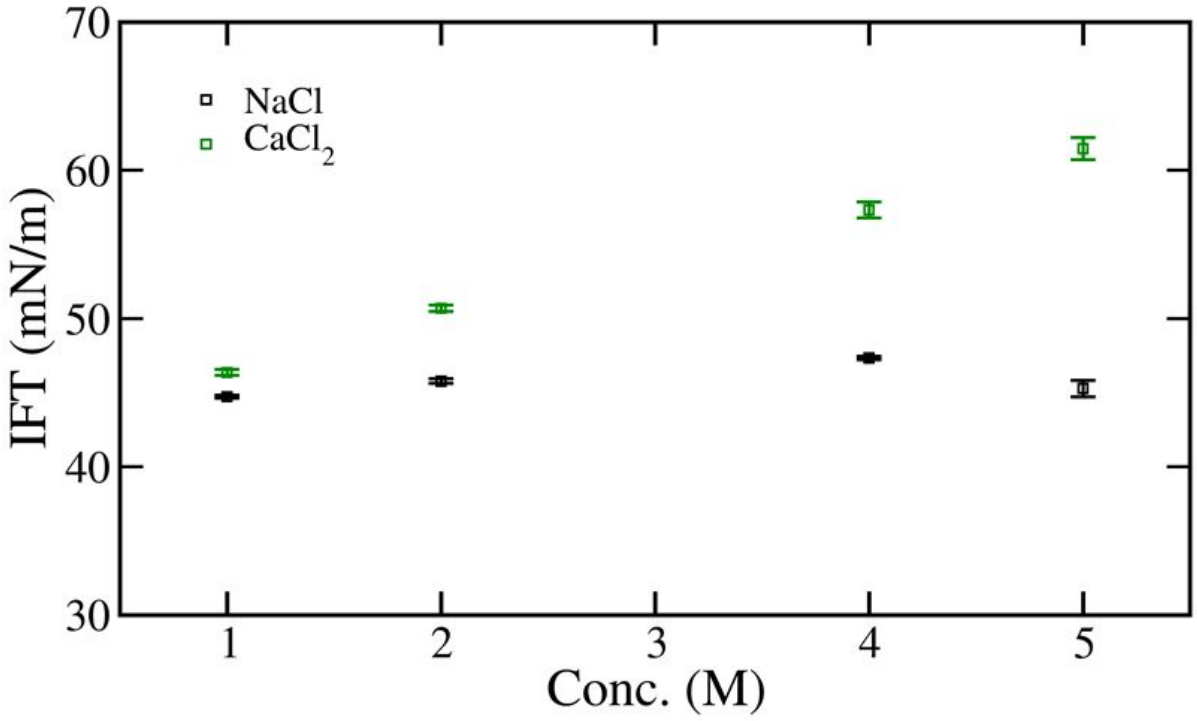

Figure S31: IFT of oil-brine for NaCl, and CaCl2 at different concentrations without the organic acids.

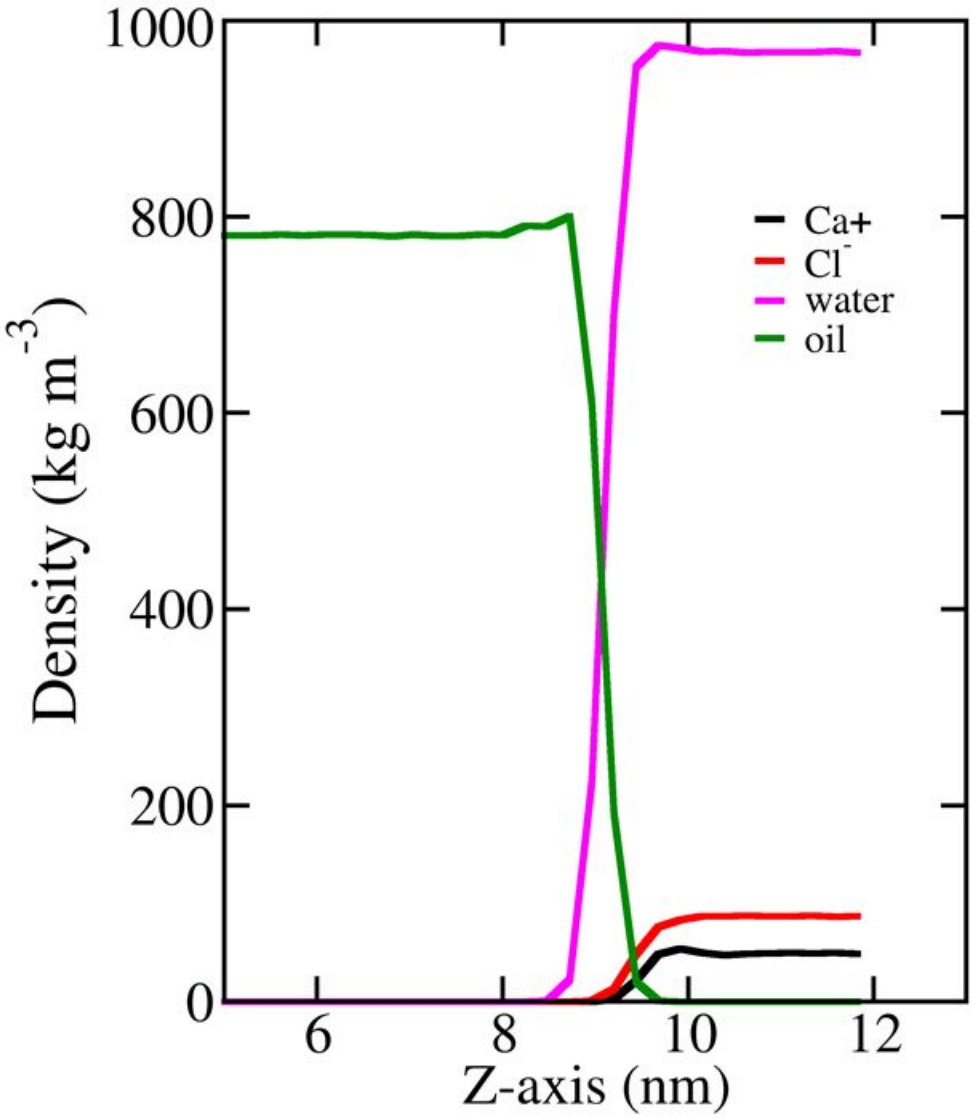

Figure S32: The partial density of the main componenents of the two phases in the xy plane and is averaged along the z-axis for oil-brine of $CalCl_2$ 1M in absence of the organic acids.